INSTITUTE OF PHYSICS PUBLISHING JOURNAL OF PHYSICS A: MATHEMATICAL AND GENERAL

J. Phys. A: Math. Gen. **37** (2004) 2073–2091 PII: S0305-4470(04)67493-2

Instability of one-step replica-symmetry-broken phase in satisfiability problems

Andrea Montanari[1], **Giorgio Parisi**[2] **and Federico Ricci-Tersenghi**[2]

[1] Laboratoire de Physique Théorique de l'Ecole Normale Supérieure (UMR 8549, Unité Mixte de Recherche du Centre National de la Recherche Scientifique et de l'Ecole Normale Supérieure), 24, rue Lhomond, 75231 Paris Cedex 05, France
[2] Dipartimento di Fisica, INFM (UdR and SMC centre) and INFN, Università di Roma 'La Sapienza', Piazzale Aldo Moro 2, I-00185 Roma, Italy

Received 8 August 2003, in final form 24 November 2003
Published 28 January 2004
Online at stacks.iop.org/JPhysA/37/2073 (DOI: 10.1088/0305-4470/37/6/008)

Abstract

We reconsider the one-step replica-symmetry-breaking (1RSB) solutions of two random combinatorial problems: k-XORSAT and k-SAT. We present a general method for establishing the stability of these solutions with respect to further steps of replica-symmetry breaking. Our approach extends the ideas of Montanari and Ricci-Tersenghi (2003 *Eur. Phys. J.* B **33** 339) to more general combinatorial problems. It turns out that 1RSB is *always* unstable at sufficiently small clause density α or high energy. In particular, the recent 1RSB solution to 3-SAT is unstable at zero energy for $\alpha < \alpha_{\mathrm{m}}$, with $\alpha_{\mathrm{m}} \approx 4.153$. On the other hand, the SAT–UNSAT phase transition seems to be correctly described within 1RSB.

PACS numbers: 75.10.Nr, 89.20.Ff, 05.70.Fh, 02.70.−c

1. Introduction

It is well known that there are two possible structures for the low-temperature phase of mean-field spin glasses [2]. The first scenario is described, within replica theory, by a one-step replica-symmetry-breaking (1RSB) ansatz. It corresponds to the existence of an exponential number of pure states which are, roughly speaking, uncorrelated. In the second scenario, a large number[3] of pure states are organized in an ultrametric tree. The tree describes the probabilistic dependences among the free energies and the distances of different pure states. This probabilistic structure corresponds, in replica jargon, to a full replica-symmetry-breaking (FRSB) ansatz.

In the last 20 years many combinatorial problems have been successfully analysed using the well-known mapping onto disordered statistical physics models [2, 3]. The same two scenarios are expected to be present within this domain. However, because of the rich

[3] An estimate of their number is still a matter of debate. See [25–27] for some recent contributions.

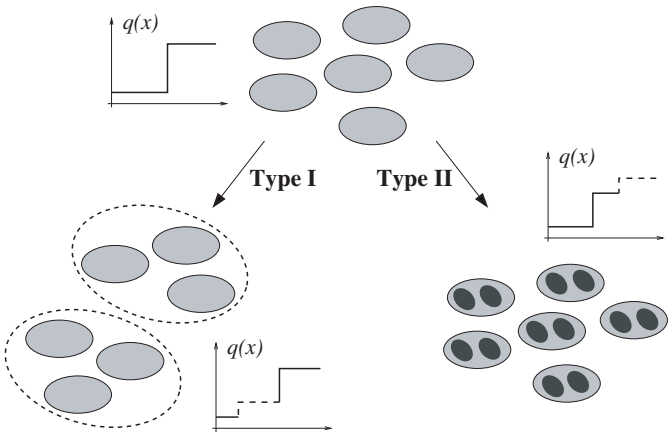

Figure 1. A pictorial view of the two types of instabilities of the 1RSB solution. Blobs represent pure states or clusters of states.

structure of many combinatorial problems, their analysis has been so far limited to 1RSB calculations. It is therefore of the utmost importance to analyse the consistency of the 1RSB solutions. An important check consists in looking at a neighbourhood of the 1RSB subspace (in the larger FRSB space) and verify the 'local stability' of the 1RSB solution.

Such a computation has recently acquired a further reason for interest. As shown in [1], even in situations in which the equilibrium behaviour is correctly treated within a 1RSB ansatz, non-equilibrium properties generically require an FRSB description. In fact, it turns out that high-lying metastable states are unstable towards FRSB. In a combinatorial optimization context 'equilibrium properties' are related to the cost of the optimal solution. 'Metastable states' are, possibly, related to the dynamics of local search algorithms [4].

There are two possible instabilities of the 1RSB calculation [1]. If we think of the 1RSB solution as describing the decomposition of the Gibbs measure in many, well-separated pure states, the following scenarios are possible: (I) the states organize themselves into clusters, forming an ultrametric FRSB structure; (II) each state splits into many sub-states forming an FRSB structure. In figure 1 we present a pictorial interpretation of these two instabilities. Type-I instability usually occurs at low energy, and often below the ground-state energy. In this case it is irrelevant from a statistical physics point of view. The calculation of [5] for 3-SAT was related to type-I instability, and confirmed the irrelevance of this phenomenon. Type-II instability affects always the high-lying metastable states and, in some regions of the phase diagram, even the ground state. Here we shall compute the threshold for this type of instability.

In this paper, we shall focus on satisfiability problems, and in particular treat the special cases of k-XORSAT and k-SAT. These are problems in which a large number of Boolean variables have to be fixed in such a way that a set of constraints (clauses) are satisfied. k-SAT lies at the very heart of theoretical computer science. It is, in fact, one of the first problems which has been proved to be NP-complete (the first being its irregular version: SAT) [6]. Much effort has been devoted to the study of the SAT–UNSAT transition in random k-SAT [7, 8]. The 1RSB solution of this model has been a quite recent achievement [9, 10]. k-XORSAT is somehow simpler than k-SAT (both from the analytic and the algorithmic points of view), while sharing a similar phase diagram [11, 12]. Interestingly, its 1RSB solution has been proved to be correct in the zero-energy limit [13, 14].

Since we are mainly interested in combinatorial problems, we shall focus on zero-temperature statistical mechanics. In the main part of our paper we fix $T = 0$ from the beginning of our calculations. It is however instructive to solve the problem (in the 1RSB approximation) at finite temperature and let $T \to 0$ afterwards. It turns out that the instability of the $T = 0$ 1RSB solution is reflected in an unphysical behaviour of the finite-temperature solution in the $T \to 0$ limit. This provides a useful check of our calculations.

The paper is organized as follows. In section 2 we explain how the instability of the 1RSB phase can be derived from an analysis of the two-step replica-symmetry-breaking (2RSB) saddle-point equations. We describe our method for a general satisfiability model. In section 3 we specialize to two prototypical cases, random k-XORSAT and random k-SAT, and show the results of a numerical evaluation of the stability condition. We discuss the consequences of our findings. In section 4 we consider the finite-temperature 1RSB solution. We compare the behaviour of this solution in the $T \to 0$ limit and the stability thresholds computed in the previous section. In appendix A we collect the explicit formulae for the stability of k-XORSAT and k-SAT. Finally in appendix B we expand around the dynamical transition of k-XORSAT, in order to have an analytical characterization of this transition.

2. The general approach

In this section we consider a general model over N Ising spins $\sigma_i = \pm 1$, $i \in \{1, \ldots, N\}$. The Hamiltonian is the sum of $M = \alpha N$ terms, each one being a k-spin interaction (we shall be interested in the case $k \geqslant 3$). We use the indices $a, b, c, \ldots \in \{1, \ldots, M\}$ for the interactions, and denote by $\partial a = \left\{i_1^a, \ldots, i_k^a\right\}$ the set of sites entering in the interaction a. Conversely ∂i will be the set of interactions in which i participates. With these conventions the Hamiltonian reads

$$H(\underline{\sigma}) = \sum_{a=1}^{M} E_a(\underline{\sigma}_{\partial a}) \tag{1}$$

where we used the vector notation $\underline{\sigma} = (\sigma_1, \ldots, \sigma_N)$ and $\underline{\sigma}_{\partial a} = \left(\sigma_{i_1^a}, \ldots, \sigma_{i_k^a}\right)$. The functions $E_a(\cdot)$ may (eventually) depend upon some quenched random variables which we will not note explicitly. Each interaction (clause) $E_a(\cdot)$ can take two values: either 0 (the clause is satisfied) or 2 (unsatisfied).

A nice graphical representation of such a model is obtained by drawing a factor graph [15], cf figure 2. This is a bipartite graph with two types of nodes: variable nodes and clause nodes. An edge is drawn between the clause a and the variable i if $i \in \partial a$ (or, equivalently, $a \in \partial i$). A crucial property for mean-field theory to be exact is that the factor graph must not contain 'short' loops.

Let $\mathcal{S}$ be the space of probability distribution $\rho \equiv (\rho_+, \rho_0, \rho_-)$ over the set $\{+, 0, -\}$. Geometrically $\mathcal{S}$ is the two-dimensional simplex. The zero-temperature 2RSB order parameter for the model (1) is given by a distribution over $\mathcal{S}$ for each *directed* link of the factor graph. We shall denote such distributions by $Q_{i\to a}[\rho]$ (if the link is directed from a variable node to a clause node) or by $\hat{Q}_{a\to i}[\hat{\rho}]$ (in the opposite case). The 2RSB cavity equations for such a model have the general form

$$Q_{i\to a}[\rho] = \frac{1}{\mathcal{Z}} \int \prod_{b\in\partial i\setminus a} \mathrm{d}\hat{Q}_{b\to i}[\hat{\rho}^{(b)}] z[\{\hat{\rho}^{(b)}\}; \mu_2]^{\mu_1/\mu_2} \delta[\rho - \rho^{\mathrm{c}}[\{\hat{\rho}^{(b)}\}; \mu_2]] \tag{2}$$

$$\hat{Q}_{a\to i}[\hat{\rho}] = \int \prod_{j\in\partial a\setminus i} \mathrm{d}Q_{j\to\alpha}[\rho^{(j)}] \delta[\hat{\rho} - \hat{\rho}^{\mathrm{c}}[\{\rho^{(j)}\}]] \tag{3}$$

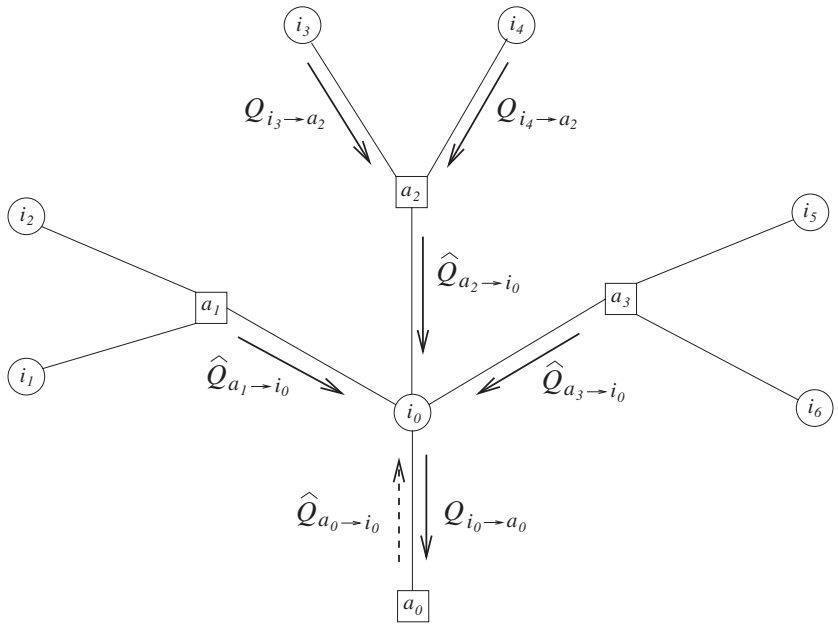

Figure 2. A fragment of a factor graph. Squares represent clauses (interactions) and circles represent variables (spins). Variable nodes are connected by a link to the clauses they belong to. Cavity fields (and their distributions) are associated with directed edges.

where μ_1 and μ_2 are the zero-temperature Parisi parameters and satisfy the usual inequalities $0 \leqslant \mu_1 \leqslant \mu_2$. They are related to their finite-temperature counterparts m_1 and m_2 as follows: $\mu_i = \lim_{T\to 0} m_i(T)/T$. The integrals in equations (2), (3) run over the simplex $\mathcal{S}$. The delta-functions are understood to operate on the same space. Note that, with respect to the 2RSB equations used in [1], we allowed for a site dependence of the order parameter. This is necessary when dealing with locally heterogeneous models such as those treated in this paper.

The function $\hat{\rho}^{\rm c}[\rho^{(1)}\dots\rho^{(k-1)}]$ (here 'c' stands for 'cavity') is model dependent. We will recall in appendix A its precise form for the models treated in section 3. The functions $\rho^{\rm c}[\hat{\rho}^{(1)}\dots\hat{\rho}^{(l)};\mu_2]$ and $z[\hat{\rho}^{(1)}\dots\hat{\rho}^{(l)};\mu_2]$ are, on the other hand, universal. They are defined as follows:

$$\rho^{\rm c}_q = \frac{1}{z[\{\hat{\rho}^{(i)}\};\mu_2]} \sum_{(q_1\dots q_l)\in\Omega_q} \prod_{i=1}^{l} \hat{\rho}^{(i)}_{q_i}\, {\rm e}^{-\mu_2(\sum_i |q_i| - |\sum_i q_i|)} \qquad q\in\{+,0,-\} \tag{4}$$

where $\Omega_+ = \{(q_1\dots q_l) : \sum_i q_i > 0\}$, $\Omega_0 = \{(q_1\dots q_l) : \sum_i q_i = 0\}$, and $\Omega_- = \{(q_1\dots q_l) : \sum_i q_i < 0\}$ (with $q_i \in \{+,0,-\}$). The normalization $z[\{\hat{\rho}^{(i)}\};\mu_2]$ is fixed by requiring $\rho^{\rm c}_+ + \rho^{\rm c}_0 + \rho^{\rm c}_- = 1$. Hereafter we will use the symbols $q, q_i, q', \dots$ for variables running over the set $\{+,0,-\}$.

In order to select a type-II instability [1], see section 1, we shall consider order parameters which concentrate near the 'corners' of the simplex $\mathcal{S}$: $\delta^{(+)}$, $\delta^{(0)}$, $\delta^{(-)}$. The corner distributions are defined by $\delta^{(q)}_{q'} = 1$ if $q = q'$ and 0 otherwise. We can decompose such order parameters as follows:

$$Q_{i\to a}[\rho] = r^{(+)}_{i\to a} Q^{(+)}_{i\to a}[\rho] + r^{(0)}_{i\to a} Q^{(0)}_{i\to a}[\rho] + r^{(-)}_{i\to a} Q^{(-)}_{i\to a}[\rho] \tag{5}$$

$$\hat{Q}_{a\to i}[\hat{\rho}] = \hat{r}^{(+)}_{a\to i} \hat{Q}^{(+)}_{a\to i}[\hat{\rho}] + \hat{r}^{(0)}_{i\to a} \hat{Q}^{(0)}_{a\to i}[\hat{\rho}] + \hat{r}^{(-)}_{i\to a} \hat{Q}^{(-)}_{a\to i}[\hat{\rho}] \tag{6}$$

where the distributions $Q^{(q)}_{i\to a}[\rho]$ and $\hat{Q}^{(q)}_{a\to i}[\hat{\rho}]$ are supposed to be normalized and concentrated near $\delta^{(q)}$. We parametrize the 'width' of these distributions using the six parameters for each directed link:

$$\epsilon^{(q)+}_{i\to a} \equiv (-1)^{\delta_{q,+}} \int \mathrm{d}Q^{(q)}_{i\to a}[\rho]\big(\rho_+ - \delta^{(q)}_+\big) \qquad \epsilon^{(q)-}_{i\to a} \equiv (-1)^{\delta_{q,-}} \int \mathrm{d}Q^{(q)}_{i\to a}[\rho](\rho_- - \delta^{(q)}_-) \quad (7)$$

with analogous definitions for the parameters $\hat{\epsilon}^{(q)+}_{a\to i}$ and $\hat{\epsilon}^{(q)-}_{a\to i}$. Note that the $(-1)^{\delta_{q,\cdot}}$ prefactors have been properly chosen to make the $\epsilon^{(q)\sigma}_{i\to a}$, $\hat{\epsilon}^{(q)\sigma}_{a\to i}$ positive.

It is easy to see that the recursions (2), (3) preserve the subspace $\{Q, \hat{Q} : \epsilon^{(q)\pm}_{i\to a} = \hat{\epsilon}^{(q)\pm}_{a\to i} = 0$ for any $i, a, q\}$. This is in fact a possible embedding of the 1RSB solution in the 2RSB space. Of course the parameters $r^{(q)}_{i\to a}$ and $\hat{r}^{(q)}_{a\to i}$ must satisfy, in this case, the 1RSB equations:

$$r_{i\to a} = \rho^{\mathrm{c}}[\{\hat{r}_{b\to i}\}_{b\in\partial i\setminus a}; \mu_1] \qquad \hat{r}_{a\to i} = \hat{\rho}^{\mathrm{c}}[\{r_{j\to a}\}_{j\in\partial a\setminus i}]. \quad (8)$$

In order to check the stability of the 1RSB subspace, we must linearize equations (2) and (3) for small $\epsilon^{(q)\pm}_{i\to a}$, $\hat{\epsilon}^{(q)\pm}_{a\to i}$. This yields equations of the form

$$\epsilon^{(q)\sigma}_{i\to a} \approx \sum_{b\in\partial i\setminus a} \sum_{q',\sigma'} T^{(a)}_{b\to i}(q,\sigma|q',\sigma')\hat{\epsilon}^{(q')\sigma'}_{b\to i} \quad (9)$$

$$\hat{\epsilon}^{(q)\sigma}_{a\to i} \approx \sum_{j\in\partial a\setminus i} \sum_{q',\sigma'} \hat{T}^{(i)}_{j\to a}(q,\sigma|q',\sigma')\epsilon^{(q')\sigma'}_{j\to a} \quad (10)$$

where $\sigma, \sigma' \in \{+,-\}$. The 6×6 matrices $T^{(a)}_{b\to i}$ and $\hat{T}^{(i)}_{j\to a}$ can be computed in terms of the cavity functions $\rho^{\mathrm{c}}[\cdots]$, $\hat{\rho}^{\mathrm{c}}[\cdots]$ and of the 1RSB solution, cf equation (8). For instance, expanding equation (2) we get

$$T^{(a)}_{b\to i}(q,\sigma|q',\sigma') = \frac{1}{z_q[\{\hat{r}_{c\to i}\};\mu_1]} \sum_{\substack{\{q_c\}\in\Omega_q \\ q_b=q'}} \prod_{c\in\partial i\setminus a} \hat{r}^{(q_c)}_{c\to i}\, \mathrm{e}^{-\mu_1(\sum_c|q_c|-|\sum_c q_c|)} M^{(b)}_{\sigma,\sigma'}(\{q_c\};\mu_2) \quad (11)$$

where

$$z_q[\{\hat{r}_{c\to i}\};\mu_1] \equiv \sum_{\{q_c\}\in\Omega_q} \prod_{c\in\partial i\setminus a} \hat{r}^{(q_c)}_{c\to i}\, \mathrm{e}^{-\mu_1(\sum_c|q_c|-|\sum_c q_c|)}. \quad (12)$$

The matrix $M^{(b)}_{\sigma,\sigma'}(\{q_c\};\mu_2)$ is obtained by linearizing the cavity function $\rho^{\mathrm{c}}[\hat{\rho}^{(1)}\ldots\hat{\rho}^{(l)};\mu_2]$, cf equation (4), near the corners of the simplex:

$$M^{(i)}_{\sigma,\sigma'}(q_1\ldots q_l;\mu_2) \equiv \left|\frac{\partial\rho^{\mathrm{c}}_\sigma}{\partial\hat{\rho}^{(i)}_{\sigma'}} - \frac{\partial\rho^{\mathrm{c}}_\sigma}{\partial\hat{\rho}^{(i)}_0}\right|_{\hat{\rho}^{(i)}=\delta^{(q_i)}}. \quad (13)$$

Note that expression (11) depends explicitly both on μ_1 and μ_2, and, through $\hat{r}^{(q)}_{a\to i}$, on μ_1. However, it can be shown that the dependence on μ_2 cancels if the stability condition is considered. We can therefore identify μ_1 with the 1RSB parameter μ.

Let us now discuss how equations (9), (10) can be used to determine whether the 1RSB solution is stable. The idea is to implement these recursions, together with equation (8), as a message-passing algorithm [16]. One keeps in memory the value of the 1RSB order parameter $r_{i\to a}$ (or $\hat{r}_{a\to i}$) and of the six fluctuation parameters $\epsilon^{(q)\sigma}_{i\to a}$ (or $\hat{\epsilon}^{(q)\sigma}_{a\to i}$) for each directed link. At each iteration these values are updated using equations (8)–(10) for all the links of the graph (one should imagine the old values to be used on the right-hand side and the new ones coming out on the left-hand side). The matrices $T^{(a)}_{b\to i}$ and $\hat{T}^{(i)}_{j\to a}$ must be recomputed after each sweep

in terms of the most recent values of $r_{i\to a}$ and $\hat{r}_{a\to i}$. After a fast transient the numbers $r_{i\to a}$ and $\hat{r}_{a\to i}$ converge to the 1RSB solution. As for the $\epsilon_{i\to a}^{(q)\sigma}$ and $\hat{\epsilon}_{a\to i}^{(q)\sigma}$, either they converge to 0 or they stay different from 0 (and, in fact, diverge). In the first case the 1RSB solution is stable, in the second one it is unstable.

The above procedure can be improved in several aspects. First of all one can define (and monitor) an appropriate norm of the ϵ, e.g.

$$\|\epsilon\| = \frac{1}{N}\sum_{i=1}^{N}\sum_{a\in\partial i}\sum_{q,\sigma}\left|\epsilon_{i\to a}^{(q)\sigma}\right|. \tag{14}$$

After each updating sweep one can renormalize the ϵ by setting $\lambda = \|\epsilon\|$ and $\epsilon_{i\to a}^{(q)\sigma} \leftarrow \epsilon_{i\to a}^{(q)\sigma}/\lambda$. The 1RSB solution is stable if $\lambda < 1$, and unstable otherwise. It is evident that λ converges to the largest eigenvalue of the linear transformation (9), (10). The determination of the 'stability parameter' λ can be improved by averaging it over many iterations of the algorithm.

In the following sections we will be interested in evaluating the stability threshold for *ensembles* of models. In this case one can implement the same algorithm as before drawing the local structure of the graph randomly at each iteration [17]. Moreover, by cleverly exploiting the structure of the model to be studied, one can reduce the number of fluctuation parameters $\epsilon, \hat{\epsilon}$ per link. In both the examples to be studied below, it is possible to use just one parameter ϵ and one $\hat{\epsilon}$ per link.

As a final remark, let us note that the method outlined in this section for $T = 0$, can be generalized to finite-temperature calculations [18].

3. Numerical evaluation of the stability condition

In this section we treat two *ensembles* of satisfiability models having Hamiltonians of the form (1): random k-XORSAT and random k-SAT. In both cases the k-uple of sites $\left(i_1^a \dots i_k^a\right)$ involved in a given clause a is chosen with flat probability distribution among the $\binom{N}{k}$ possible k-uples.

The zero-temperature phase diagram of these models (for $k \geqslant 3$) is known [7–10, 12–14] to be composed of three different phases as a function of α, cf figures 3 and 4. For $\alpha < \alpha_{\rm d}$ the system is paramagnetic with no diverging energy barriers in the configurational space. For $\alpha_{\rm d} \leqslant \alpha \leqslant \alpha_{\rm c}$ the model is still unfrustrated: the ground-state energy is zero. Nevertheless the Gibbs measure decomposes in an exponentially large number of pure states separated by large energy barriers. For $\alpha > \alpha_{\rm c}$ frustration percolates and the ground-state energy becomes positive. The ground state is still hidden within a large number of metastable states.

Within the 1RSB approximation, the system is completely described by the complexity $\Sigma(e)$, i.e. the normalized logarithm of the number of metastable states with energy density e. For $\alpha > \alpha_{\rm d}$, the complexity becomes strictly positive in the interval $e \in [e_{\rm s}(\alpha), e_{\rm d}(\alpha)]$. The static energy $e_{\rm s}(\alpha)$ vanishes for $\alpha \leqslant \alpha_{\rm c}$ and becomes positive above the static transition point $\alpha_{\rm c}$. The 1RSB dynamical energy $e_{\rm d}$, becomes positive at the dynamical critical point $\alpha_{\rm d}$. Following the prescription of [19], the 1RSB complexity can be obtained by Legendre transforming the m-replicas free energy. We refer to appendix B for an example of this type of calculation.

The 1RSB calculation of $\Sigma(e)$ becomes quite generally [1] unstable with respect to further replica-symmetry breakings above the Gardner energy $e_{\rm G}$, with $e_{\rm G} < e_{\rm d}$. We expect the 1RSB result to be correct only for $e \leqslant e_{\rm G}$. In the following we shall present our results for $e_{\rm G}(\alpha)$ obtained with the method outlined in the previous section.

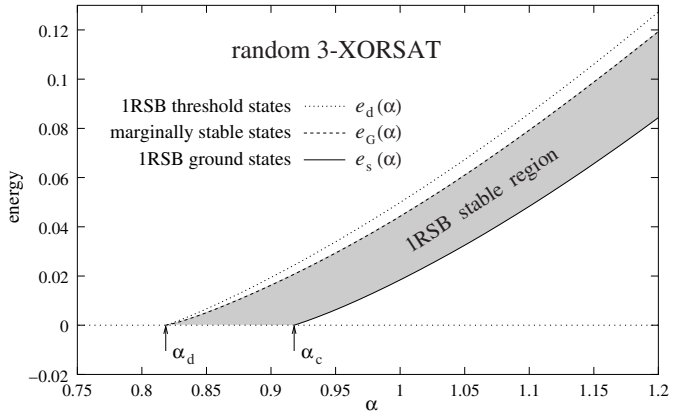

Figure 3. The stability region in the energy-clause density plane for 3-XORSAT. We used population dynamics algorithms with $O(10^5)$ elements and $O(10^2)$ iterations. The marginal stability line $e_G(\alpha)$ crosses the one-step ground-state energy $e_s(\alpha)$ at $\alpha_G = 3.072(2)$ (outside the range shown here).

3.1. k-XORSAT

The definitions given so far are completed by taking

$$E_a(\underline{\sigma}_{\partial a}) = 1 - J_a \sigma_{i_1^a} \cdots \sigma_{i_k^a} \tag{15}$$

where the J_a are i.i.d. (quenched) random variables taking the values ± 1 with equal probabilities. We recall [11, 12] that the existence of an unfrustrated ground state can be mapped onto the existence of a solution for a certain random linear system over $G\mathbb{F}$ [2].

In figure 3 we present our results for the zero-temperature phase diagram for $k = 3$ (but the picture remains qualitatively similar for any k). For $k = 3$ we have $\alpha_d \approx 0.818\,469\,16$ and $\alpha_c \approx 0.917\,935\,28$. It is evident from the data of figure 3 that $0 < e_G(\alpha) < e_d(\alpha)$ for $\alpha > \alpha_d$, and that $e_G(\alpha), e_d(\alpha) \downarrow 0$ as $\alpha \downarrow \alpha_d$. This is confirmed by a perturbative expansion for $\alpha \to \alpha_d$, cf appendix B. In particular we get

$$e_d(\alpha) = e_d^{(0)}(\alpha - \alpha_d)^{1/2} + O(\alpha - \alpha_d) \qquad e_G(\alpha) = e_G^{(0)}(\alpha - \alpha_d) + O((\alpha - \alpha_d)^{3/2}) \tag{16}$$

with $e_d^{(0)} \approx 0.010\,750\,6548$ and $e_G^{(0)} \approx 0.075\,398\,7711$ for $k = 3$. Let us stress that our result $e_G(\alpha) > 0$ for $\alpha > \alpha_d$ is consistent with the rigorous solution of the model at $e = 0$ [13, 14].

In the limit $\alpha \to \infty$ we expect to recover the fully connected k-spin Ising spin glass. At zero temperature this model is characterized by FRSB even for what concerns the ground state [20]. This implies that the line $e_G(\alpha)$ must cross $e_s(\alpha)$ at some finite α_G. This expectation is in fact fulfilled by our data: we get $\alpha_G = 3.072(2)$ for $k = 3$. For $\alpha > \alpha_G$ the 1RSB result for the ground-state energy is just a lower bound [21].

3.2. k-SAT

In this case the energy of a clause is

$$E_a(\underline{\sigma}_{\partial a}) = 2 \prod_{i \in \partial a} \frac{1 - J_{a \to i}\sigma_i}{2} \tag{17}$$

where the $J_{a\to i}$ are i.i.d. (quenched) random variables taking the values ± 1 with equal probabilities. The clause has energy 2 (it is not satisfied) if all participating spins σ_i have

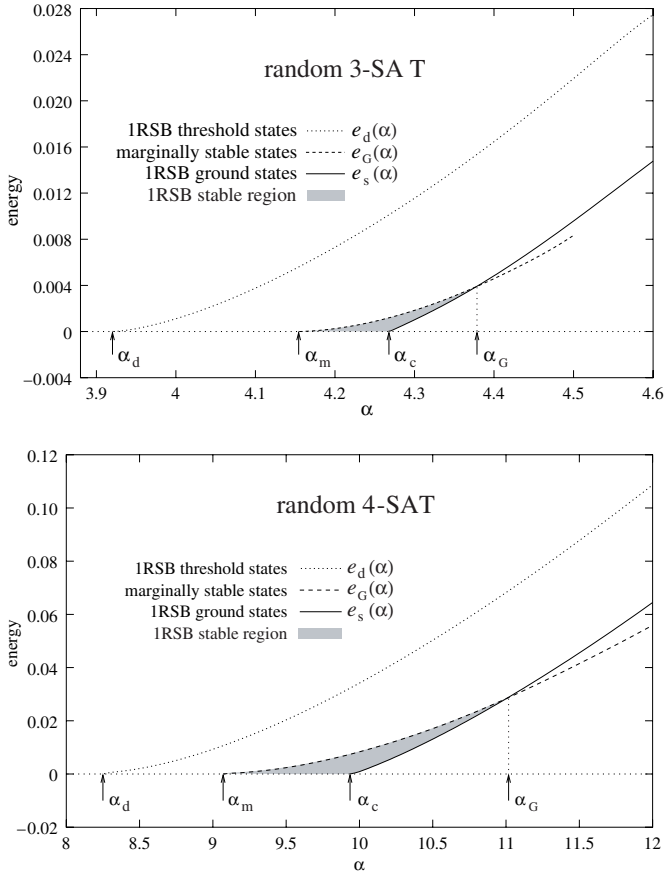

Figure 4. The stability region in the energy-clause density plane for 3-SAT (top) 4-SAT (bottom). Here we used population dynamics algorithms with (typically) $O(10^5)$ elements and $O(10^2)$ iterations.

opposite signs to the corresponding $J_{a\to i}$. In all the other cases it has energy 0 (it is satisfied). In figure 4 we show the results of our method for the stability threshold $e_G(\alpha)$, together with the curves for $e_s(\alpha)$ and $e_d(\alpha)$ computed in [9, 10]. We considered the two prototypical cases $k = 3$ and $k = 4$, but we expect the picture to remain qualitatively similar for any $k \geqslant 3$. There is an important qualitative difference with respect to k-XORSAT: for k-SAT $e_G(\alpha) \downarrow 0$ for $\alpha \downarrow \alpha_m$ with $\alpha_d < \alpha_m < \alpha_c$. In other words, even zero-energy states become unstable towards FRSB at sufficiently low α (but above α_d of course). In the 1RSB picture, zero-energy states are related to a cluster of solutions of the corresponding satisfiability problem [8–10]. It would be interesting to understand how this picture must be modified below α_m. Generalizing the ideas of [1], we expect, within a 2RSB description, such clusters to split continuously into sub-clusters at α_m.

Unlike k-XORSAT, the stability computation has a non-trivial result even at zero energy. It is therefore interesting to modify the approach of section 2 in order to consider this limit case. The zero-energy limit of the 2RSB equations (2), (3) is obtained by taking $\mu_1, \mu_2 \to \infty$ with $\mu_1/\mu_2 = x$ fixed. As already noted in section 2, the stability parameter λ ends up not depending upon μ_2, and therefore x. We report our results for $\lambda(\alpha, e = 0)$ in figure 5. This

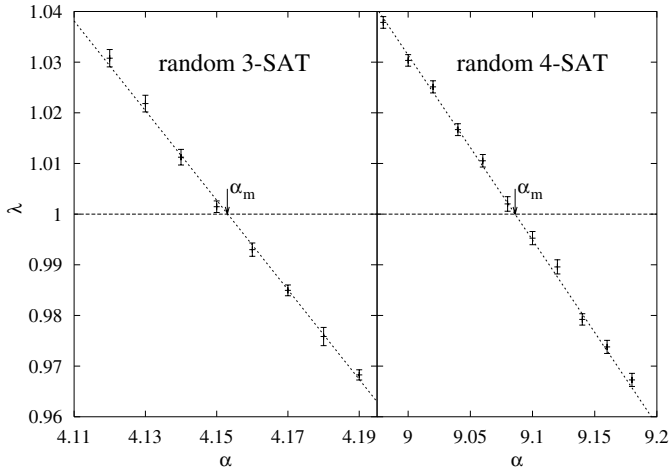

Figure 5. The stability parameter (largest eigenvalue of the stability matrix) $\lambda(\alpha, e = 0)$ for 3-SAT (left) and 4-SAT (right).

approach provides us good estimates of α_m. We get $\alpha_m = 4.153(1)$ for $k = 3$ and $\alpha_m = 9.086(2)$ for $k = 4$. This should be compared with the values $\alpha_d = 3.925(3)$ and $\alpha_c = 4.266(1)$ for $k = 3$, and $\alpha_d = 8.295(6)$ and $\alpha_c = 9.931(2)$ for $k = 4$.

Finally, in the large connectivity limit, the 1RSB solution is unstable even for the ground state. The curves $e_G(\alpha)$ and $e_s(\alpha)$ cross at α_G. We get $\alpha_G = 4.390(5)$ for $k = 3$ and $\alpha_G = 10.98(2)$ for $k = 4$.

4. On the zero-temperature limit of the 1RSB solution

In this section we consider the finite-temperature 1RSB solution and discuss its $T \to 0$ limit. At finite temperature the 1RSB order parameter is given by a probability distribution over the reals for each directed link. We shall call these distributions $\rho_{i\to a}(h)$ and $\hat{\rho}_{a\to i}(u)$. The variables u and h are 'cavity fields'. If the factor graph were a tree, we could define the cavity fields as follows. Consider the branch $a \to i$ of the graph: this is the connected sub-tree which has i as the root and contains only a among the neighbours of i. Let $Z_{a\to i}(\sigma_i)$ be the partition function for this subsystem constrained to a given value of σ_i, at inverse temperature β. This quantity can be parametrized in terms of a cavity field $u_{a\to i}$ as follows:

$$Z_{a\to i}(\sigma_i) = Z^{(0)}_{a\to i}\, \mathrm{e}^{\beta u_{a\to i}\sigma_i}. \tag{18}$$

It is now elementary to show that, if the Hamiltonian has the form (1), with $E_a(\underline{\sigma}_{\partial a})$ taking values in $\{0, 2\}$, the field $u_{\alpha\to i}$ must become an integer number when $T \to 0$. The same conclusion is easily reached for the fields $h_{i\to a}$.

The situation is less clear on locally tree-like graphs, such as those considered in section 3. However, one can argue that the same property of the $T \to 0$ limit must hold *within* each pure state. Suppose now that the finite-T 1RSB cavity field distributions $\rho_{i\to a}(h)$ or $\hat{\rho}_{a\to i}(u)$ have a non-vanishing support over non-integer fields even in the $T \to 0$ limit (the finite-temperature 1RSB equations are recalled in appendix C). It is reasonable to take this as an evidence for the 1RSB ansatz being incorrect (this kind of argument was pioneered in [22]). In fact we do not expect the properties of the system to be discontinuous at $T = 0$.

Let us note in passing that other interesting phenomena appear when $T > 0$. At infinitesimal temperature the cavity fields acquire a small part proportional to the temperature. These evanescent contributions can in turn undergo one or several replica-symmetry-breaking transitions [8]. This is what happens in 3-SAT above $\alpha_{\rm b} \approx 3.87 < \alpha_{\rm d}$ [5]. The underlying physical phenomenon is the following. In the region $\alpha_{\rm b} < \alpha < \alpha_{\rm d}$ the space of solutions decomposes into clusters. However these clusters do not have any backbone (i.e. a subset of the variables which is fixed in all solutions of the cluster). The backbone percolates at $\alpha_{\rm d}$. In this section we focus on 'hard' cavity fields (i.e. non-vanishing in the zero-temperature limit) and these effects do not concern us. Note that 'hard' fields are those determining the energy in the $T \to 0$ limit.

It is easy to understand why a cavity field distribution not concentrated on the integers in the $T \to 0$ limit, should be related to the instability of the 1RSB solution. Indeed the effect of the finite temperature is to provide fields that are not integers but differ from integers by a term of order T. When we insert these slightly non-integer fields in the cavity equations this perturbation may be amplified, and after a finite number of steps the distribution may spread over non-integer fields. This instability corresponds to the propagation of a perturbation at any distance and it is a signal of instability of the 1RSB solution.

We investigated this phenomenon analytically for k-XORSAT and k-SAT. The idea is to write the 1RSB order parameter as follows:

$$\hat{\rho}_{a\to i}(u) = \hat{r}^{(+)}_{a\to i}\delta(u-1) + \hat{r}^{(0)}_{a\to i}\delta(u) + \hat{r}^{(-)}_{a\to i}\delta(u+1) + \hat{\epsilon}^{(+)}_{a\to i}(u) + \hat{\epsilon}^{(-)}_{a\to i}(u) \tag{19}$$

and analogously for $\rho_{i\to a}(h)$, with $\hat{\epsilon}^{(+)}_{a\to i}(u), \hat{\epsilon}^{(-)}_{a\to i}(u)$ small perturbations supported, respectively over (0, 1), and $(-1, 0)$ (it turns out that $|u| \leqslant 1$ always). We then considered the $T = 0$ cavity equations with the 1RSB parameter μ. It is easy to realize that the 1RSB equations leave the $\hat{\epsilon}_{a\to i}, \epsilon_{i\to a} = 0$ subspace invariant (we worked indeed within this subspace in the rest of the paper). The next step is therefore to expand for small perturbations $\epsilon^{(\pm)}_{i\to a}(h)$ and $\hat{\epsilon}^{(\pm)}_{a\to i}(u)$. The resulting linear equations have a simple invariant subspace:

$$\hat{\epsilon}^{(\pm)}_{a\to i}(u) = \hat{\delta}^{(\pm)}_{a\to i}\, {\rm e}^{\mu|u|} \tag{20}$$

and analogously for $\epsilon^{(\pm)}_{i\to a}(h)$ (with parameters $\delta^{(\pm)}_{i\to a}$). One can therefore deduce a set of linear recursions for the parameters $\hat{\delta}^{(\pm)}_{a\to i}$, $\delta^{(\pm)}_{i\to a}$. It turns out that, both for k-SAT and for k-XORSAT, these recursions are equivalent to those obtained in the previous sections for the 2RSB perturbations. Under the assumption that equation (20) defines the most relevant (unstable) subspace, this implies that stability with respect to non-integer fields is indeed equivalent to stability with respect to 2RSB perturbations.

For finite μ, we analysed this instability numerically. As an example, in figure 6 we report the results of a numerical solution of the 1RSB equations for 3-SAT at $\alpha = 4.51 > \alpha_{\rm G}$. Here we used $T = 10^{-5}$ and the 1RSB parameter $\mu = 1.75$ and 2.25, which should be confronted with the ground-state value $\mu_{\rm s}(\alpha = 4.51) = 1.94(1)$. The first choice of μ corresponds to metastable states, while the second to an energy below the ground state. It is clear from the figure that $\mu = 1.75$ is in the unstable region while $\mu = 2.25$ is in the stable region.

In fact the distributions $\rho_{i\to a}(h)$ or $\hat{\rho}_{a\to i}(u)$ acquire a non-vanishing support on non-integer fields as soon as $\mu < \mu_{\rm int}(\alpha)$ (i.e. for energy $e > e_{\rm int}(\alpha)$). A precise numerical determination of $\mu_{\rm int}(\alpha)$ is not simple because finding the solution of the cavity equations at finite temperature is a rather slow process. Moreover many systematic effects must be taken into account. As mentioned above consistency implies that $\mu_{\rm int}(\alpha) \leqslant \mu_{\rm G}(\alpha)$. Furthermore, we argued $\mu_{\rm int}(\alpha) = \mu_{\rm G}(\alpha)$ under the assumption that equation (20) defines indeed the most relevant perturbation. Our best numerical estimates give $\mu_{\rm int}(4.51) = 2.00(3)$. This

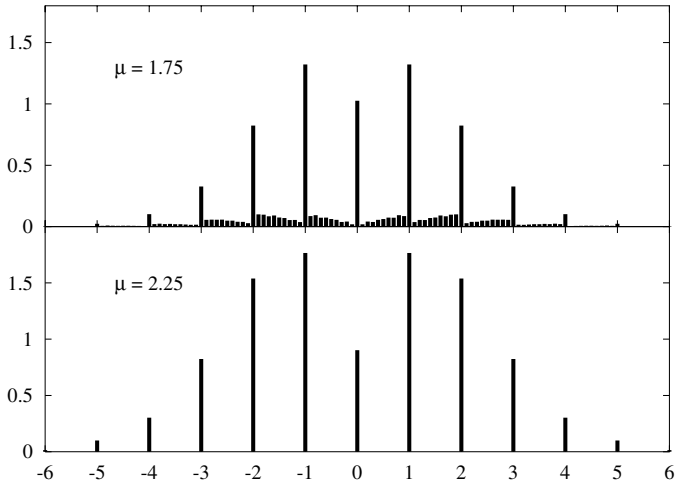

Figure 6. Cavity field distribution $\rho_{i\to a}(h)$ of 3-SAT, averaged over all the directed links of the factor graph. Here we used $\mu = 1.75$ (upper frame) and 2.25 (lower frame), and $\alpha = 4.51$. The 1RSB equations were solved by a population dynamics algorithm with 4000 populations of 256 fields each.

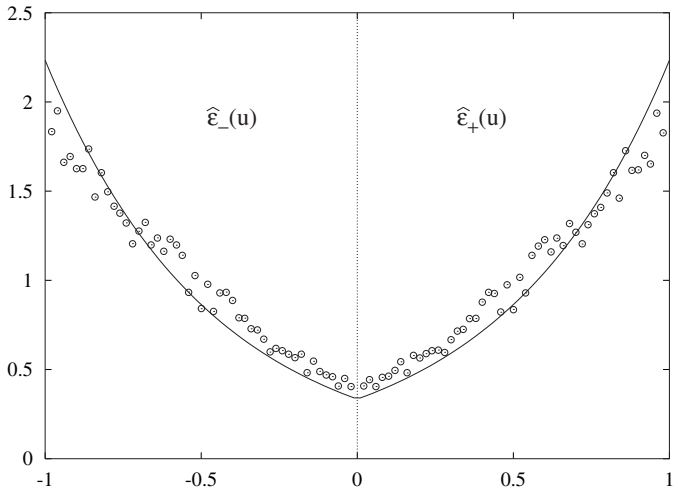

Figure 7. Distributions $\hat{\epsilon}^{(\pm)}_{a\to i}(u)$ of non-integer cavity fields for 3-SAT, averaged over all the directed links of the factor graph. Here we used $\alpha = 4.51$ and $\mu = 1.9 < \mu_{\rm int}$ and normalized the integral of $\hat{\epsilon}^{(\pm)}_{a\to i}(u)$ to 1. The continuous line corresponds to the theoretical expectation $C\exp(\mu|u|)$, cf equation (20). The constant $C \approx 0.334$ is fixed by the normalization condition.

is numerically compatible with the result obtained with the methods of sections 2 and 3: $\mu_{\rm G}(4.51) = 2.045(5)$.

Finally in figure 7 we present our numerical data for the average of the distributions $\hat{\rho}_{a\to i}(u)$ at $\alpha = 4.51$ and $\mu = 1.9 < \mu_{\rm int}(\alpha)$. If the analytical argument outlined above is correct and in the approximation that $|\mu_{\rm int} - \mu| \approx 0.10 \ll 1$, we should have $\overline{\hat{\epsilon}^{(\pm)}_{a\to i}(u)} \approx \hat{\delta}_* \exp(\mu|u|)$. The reasonable agreement confirms that equation (20) corresponds to the most relevant subspace for finite-T perturbations.

5. Conclusion

Our main conclusion is that FRSB plays an important role in random combinatorial optimization problems such as k-XORSAT and k-SAT. We investigated this issue by analysing the stability of the cavity recursions, both within a 2RSB ansatz, cf sections 2 and 3, and at finite temperature, cf section 4.

The 1RSB ground state becomes unstable in two different regimes. In the UNSAT region, it becomes unstable in highly constrained problems: $\alpha > \alpha_{\rm G}$, i.e. when the corresponding factor graph has large connectivity. This result was not unexpected. As shown in [20] (for k-XORSAT) and [23, 24] (for 3-SAT), in the $\alpha \to \infty$ limit, these models have a low-temperature FRSB phase. In the SAT region there is an exponential number of unfrustrated ground states (i.e. solutions of the satisfiability problem). The 1RSB solution indicates that these solutions have a clustered structure in the region $\alpha_{\rm d} < \alpha < \alpha_{\rm c}$. However, this solution becomes unstable in the underconstrained region $\alpha_{\rm d} < \alpha < \alpha_{\rm m}$. Providing a more refined description of the space of solutions in this regime is an open problem (which will require presumably FRSB).

Let us recall that high-lying metastable states are *always* unstable against FRSB. This could have remarkable consequences on the performances of local search algorithms (such as simulated annealing). Let us suppose, just to estimate how large this effect can be, that there are no metastable states above the instability energy $e_{\rm G}(\alpha)$. This would imply that the total number of metastable states at the SAT–UNSAT phase transition is $\Sigma(e_{\rm G}(\alpha_{\rm c}), \alpha_{\rm c}) \approx 0.0019$ (for 3-SAT) and 0.0099 (for 4-SAT), instead of $\Sigma(e_{\rm d}(\alpha_{\rm c}), \alpha_{\rm c}) \approx 0.010$ (for 3-SAT) and 0.029 (for 4-SAT). In other words metastability would start having some effect only at much larger sizes.

In this work we studied the stability of the 1RSB phase, by analysing the stability of the cavity recursions with respect to two types of perturbations. In sections 2 and 3 we considered a perturbation towards 2RSB, while in section 4 we used a perturbation towards non-integer fields. We argued that the two approaches indeed give coincident answers, cf section 4. This leaves open the questions whether there can be more dangerous instabilities. In replica formalism, one should diagonalize the Hessian of the free energy in the full replica space. We expect that our calculation corresponds to selecting one particular subspace. The question is whether this is the most dangerous subspace. The fact [18] that in the $\alpha \to \infty$ limit our calculation yields the replicon instability points towards a positive answer.

Acknowledgments

FRT thanks ICTP for kind hospitality during the completion of this manuscript. This work is supported in part by the European Community's Human Potential Programme under contract HPRN-CT-2002-00319, Stipco, and the ESF programme SPHINX.

Appendix A. Explicit formulae

In this appendix we give the explicit forms of the recursions (8), (9) and (10) for the models treated in section 3. Moreover we show how to reduce the size of the 6×6 matrices $T^{(a)}_{b\to i}$ and $\hat{T}^{(i)}_{j\to a}$ using the symmetries of the models. Finally, it will become evident that the stability parameter λ depends uniquely upon the smallest replica-symmetry-breaking parameter μ_1.

Before turning to the models of section 3, it is useful to compute the matrix $M^{(i)}_{\sigma,\sigma'}(q_1 \dots q_l; \mu_2)$, cf equation (11), which is model independent. We get the following

result:

$$M^{(i)}_{\sigma,\sigma'}(q_1 \dots q_l;\mu_2) = \begin{cases} 0 & \text{if} \quad \sum_{j\neq i} q_j > 1 \text{ or } < 1 \\ \mathrm{e}^{-2\mu_2}\delta_{\sigma,+}\delta_{\sigma',-} & \text{if} \quad \sum_{j\neq i} q_j = 1 \text{ and } q_i = 0,+ \\ \mathrm{e}^{2\mu_2}\delta_{\sigma,+}\delta_{\sigma',-} & \text{if} \quad \sum_{j\neq i} q_j = 1 \text{ and } q_i = - \\ \mathrm{e}^{-2\mu_2}\delta_{\sigma,-}\delta_{\sigma',+} & \text{if} \quad \sum_{j\neq i} q_j = -1 \text{ and } q_i = 0,- \\ \mathrm{e}^{2\mu_2}\delta_{\sigma,-}\delta_{\sigma',+} & \text{if} \quad \sum_{j\neq i} q_j = -1 \text{ and } q_i = + \\ \delta_{\sigma,\sigma'} & \text{if} \quad \sum_{j\neq i} q_j = 0. \end{cases} \tag{A1}$$

A.1. k-XORSAT

Let us start by recalling that the function $\hat{\rho}^{\mathrm{c}}[\rho^{(1)} \dots \rho^{(k-1)}]$ takes in this case the form

$$\hat{\rho}^{\mathrm{c}}_{+} = \frac{1}{2}\left[\prod_{i=1}^{k-1}\left(\rho^{(i)}_{+}+\rho^{(i)}_{-}\right)+\prod_{i=1}^{k-1}\left(\rho^{(i)}_{+}-\rho^{(i)}_{-}\right)\right] \tag{A2}$$

$$\hat{\rho}^{\mathrm{c}}_{0} = 1-\prod_{i=1}^{k-1}\left(\rho^{(i)}_{+}+\rho^{(i)}_{-}\right) \tag{A3}$$

$$\hat{\rho}^{\mathrm{c}}_{-} = \frac{1}{2}\left[\prod_{i=1}^{k-1}\left(\rho^{(i)}_{+}+\rho^{(i)}_{-}\right)-\prod_{i=1}^{k-1}\left(\rho^{(i)}_{+}-\rho^{(i)}_{-}\right)\right]. \tag{A4}$$

This completely specifies the 2RSB saddle-point equations (2), (3). Moreover, it turns out that the 1RSB solution is symmetric under spin inversion: $r^{(+)}_{i\to a} = r^{(-)}_{i\to a}$ and $\hat{r}^{(+)}_{a\to i} = \hat{r}^{(-)}_{a\to i}$ [14]. We can therefore parametrize it in terms of a single real number per directed link, e.g. $r^{(0)}_{i\to a}$, $\hat{r}^{(0)}_{a\to i}$. Using these simplifying features it is easy to show that the matrices $T^{(a)}_{b\to i}$, $\hat{T}^{(i)}_{j\to a}$ have the following form:

$$T^{(a)}_{b\to i} = \begin{bmatrix} C_1 & C_2 & 0 & C_3 & 0 & 0 \\ 0 & C_1 & 0 & 0 & 0 & 0 \\ 0 & 0 & C_4 & 0 & 0 & C_5 \\ C_5 & 0 & 0 & C_4 & 0 & 0 \\ 0 & 0 & 0 & 0 & C_1 & 0 \\ 0 & 0 & C_3 & 0 & C_2 & C_1 \end{bmatrix} \qquad \hat{T}^{(i)}_{j\to a} = \begin{bmatrix} 1/2 & 0 & 0 & 0 & 0 & 1/2 \\ 0 & 1/2 & 0 & 0 & 1/2 & 0 \\ 0 & 0 & \hat{C} & \hat{C} & 0 & 0 \\ 0 & 0 & \hat{C} & \hat{C} & 0 & 0 \\ 0 & 1/2 & 0 & 0 & 1/2 & 0 \\ 1/2 & 0 & 0 & 0 & 0 & 1/2 \end{bmatrix} \tag{A5}$$

where we ordered the six components as follows $(q,\sigma) = \{(+,+),(+,-);(0,+),(0,-);(-,+),(-,-)\}$. The constants $C_1,\dots,C_5$ are easily computed using equations (11) and (A1), while $\hat{C} = \hat{C}^{(i)}_{j\to a}$ is given by

$$\hat{C}^{(i)}_{j\to a} = \frac{1}{2}\frac{r^{(0)}_{j\to a}\prod_{l\in\partial a\setminus\{i,j\}}\left(1-r^{(0)}_{l\to a}\right)}{1-\prod_{l\in\partial a}\left(1-r^{(0)}_{l\to a}\right)}. \tag{A6}$$

As we already pointed out, the six-dimensional transformation defined above can be reduced thanks to the symmetries of the system. Consider indeed the following parametrization of the fluctuation variables in terms of the numbers $\delta_{i\to a}$:

$$\epsilon^{(+)+}_{i\to a} = \left(\mathrm{e}^{\mu_1-2\mu_2}/r^{(+)}_{i\to a}\right)\delta_{i\to a} \qquad \epsilon^{(+)-}_{i\to a} = 0 \tag{A7}$$

$$\epsilon^{(0)+}_{i\to a} = \left(1/r^{(0)}_{i\to a}\right)\delta_{i\to a} \qquad \epsilon^{(0)-}_{i\to a} = \left(1/r^{(0)}_{i\to a}\right)\delta_{i\to a}. \tag{A8}$$

$$\epsilon^{(-)+}_{i\to a} = 0 \qquad \epsilon^{(-)-}_{i\to a} = \left(\mathrm{e}^{\mu_1-2\mu_2}\big/ r^{(-)}_{i\to a}\right)\delta_{i\to a} \tag{A9}$$

and the analogues for $\hat{\epsilon}^{(q)\sigma}_{a\to i}$ (in terms of $\hat{\delta}_{i\to a}$). It is easy to show that the linear subspace defined in this way is preserved by the transformations (9), (10). Moreover, a numerical calculation confirms that the largest eigenvalue λ belongs to this subspace. Therefore, instead of equations (9), (10) we can iterate the simpler recursion:

$$\delta_{i\to a} = \sum_{b\in\partial i\setminus a} t^{(a)}_{b\to i}\hat{\delta}_{b\to i} \qquad \hat{\delta}_{a\to i} = \sum_{j\in\partial a\setminus i} \hat{t}^{(i)}_{j\to a}\delta_{j\to a}. \tag{A10}$$

The real numbers $t^{(a)}_{b\to i}$ and $\hat{t}^{(i)}_{j\to a}$ can be derived from the matrices $T^{(a)}_{b\to i}$ and $\hat{T}^{(i)}_{j\to a}$. The result is

$$t^{(a)}_{b\to i} = \frac{1}{z[\{\hat{r}_{c\to i};\,\mu_1]}\sum_{\{q_c\}}{}' \prod_{c\in\partial i\setminus\{a,b\}} \left(\hat{r}^{(q_c)}_{c\to i}\,\mathrm{e}^{-\mu_1|q_c|}\right) \tag{A11}$$

$$\hat{t}^{(i)}_{j\to a} = \prod_{l\in\partial a\setminus\{i,j\}} \left(1 - r^{(0)}_{l\to a}\right) \tag{A12}$$

where the sum $\sum'$ is over the $\{q_c\}$ such that $\sum_{c\in\partial i\setminus\{a,b\}} q_c = 0$ or 1, and $z[\{\hat{r}_{c\to i};\,\mu_1]$ is defined as in equation (4) and discussion below. Note that the above expression no longer depends upon μ_2.

A.2. k-SAT

Once again, the first step consists in assigning the (model-dependent) function $\hat{\rho}^{\mathrm{c}}[\rho^{(1)}\dots\rho^{(k-1)}]$ entering in equation (3). Unlike for k-XORSAT, this function depends upon the quenched variables $J_{a\to i}$. We have

$$\hat{\rho}^{\mathrm{c}}_{a\to i}(J_{a\to i}) = \prod_{j\in\partial a\setminus i} \rho_{j\to a}(-J_{a\to j}) \tag{A13}$$

$$\hat{\rho}^{\mathrm{c}}_{a\to i}(0) = 1 - \prod_{j\in\partial a\setminus i} \rho_{j\to a}(-J_{a\to j}) \tag{A14}$$

$$\hat{\rho}^{\mathrm{c}}_{a\to i}(-J_{a\to i}) = 0 \tag{A15}$$

where, for greater clarity, we used the notation $\rho(q)$ and $\hat{\rho}(q)$, instead of ρ_q and $\hat{\rho}_q$ for indicating the arguments of the distributions ρ and $\hat{\rho}$. Obviously, the 1RSB solution (8) has the property that $\hat{r}^{(q)}_{a\to i} = 0$ for $q = -J_{a\to i}$. The distributions $\hat{r}_{a\to i}$ can therefore be parametrized by giving a single real number, for instance, $\hat{r}^{(0)}_{a\to i}$.

Let us now consider the fluctuation parameters $\epsilon^{(q)\sigma}_{i\to a}$ and $\hat{\epsilon}^{(q)\sigma}_{a\to i}$. The first important observation consists in noting that, because of equations (A13)–(A15), $\hat{\epsilon}^{(q)\sigma}_{a\to i} = 0$ if $\sigma = -J_{a\to i}$ or $q = -J_{a\to i}$. Using the form of the transformation $T^{(a)}_{b\to i}$, this implies $\epsilon^{(+)-}_{i\to a} = \epsilon^{(-)+}_{i\to a} = 0$. We are therefore left with four parameters $\epsilon_{i\to a}$ and two $\hat{\epsilon}_{a\to i}$ different from zero.

In order to write explicit forms for the transformations (9) and (10), it is convenient to parametrize the remaining $\epsilon_{i\to a}$ as follows:

$$\epsilon^{(+)+}_{i\to a} = \left(\mathrm{e}^{\mu_1-2\mu_2}\big/ r^{(+)}_{i\to a}\right)\delta^{(+)+}_{i\to a} \qquad \epsilon^{(0)+}_{i\to a} = \left(1\big/ r^{(0)}_{i\to a}\right)\delta^{(0)+}_{i\to a} \tag{A16}$$

$$\epsilon^{(-)-}_{i\to a} = \left(\mathrm{e}^{\mu_1-2\mu_2}\big/ r^{(-)}_{i\to a}\right)\delta^{(-)-}_{i\to a} \qquad \epsilon^{(0)-}_{i\to a} = \left(1\big/ r^{(0)}_{i\to a}\right)\delta^{(0)-}_{i\to a}. \tag{A17}$$

Analogously we parametrize the non-zero $\hat{\epsilon}^{(q)\sigma}_{a\to i}$ in terms of $\hat{\delta}^{(q)\sigma}_{a\to i}$. We are now in a position to write the explicit form of the transformations (9), (10) in a compact form. In this case it is more convenient not to use the matrix notation. We get

$$\delta^{(+)+}_{i\to a} = \sum_{b\in\Gamma_+} t^{(a)}_{b\to i}(0)\hat{\delta}^{(+)+}_{b\to i} + \sum_{b\in\Gamma_-} t^{(a)}_{b\to i}(+1)\hat{\delta}^{(0)-}_{b\to i} \tag{A.18}$$

$$\delta^{(0)+}_{i\to a} = \sum_{b\in\Gamma_+} t^{(a)}_{b\to i}(0)\hat{\delta}^{(0)+}_{b\to i} + \sum_{b\in\Gamma_-} t^{(a)}_{b\to i}(+1)\hat{\delta}^{(-)-}_{b\to i} \tag{A19}$$

$$\delta^{(0)-}_{i\to a} = \sum_{b\in\Gamma_+} t^{(a)}_{b\to i}(-1)\hat{\delta}^{(+)+}_{b\to i} + \sum_{b\in\Gamma_-} t^{(a)}_{b\to i}(0)\hat{\delta}^{(0)-}_{b\to i} \tag{A20}$$

$$\delta^{(-)-}_{i\to a} = \sum_{b\in\Gamma_+} t^{(a)}_{b\to i}(-1)\hat{\delta}^{(+)+}_{b\to i} + \sum_{b\in\Gamma_-} t^{(a)}_{b\to i}(0)\hat{\delta}^{(-)-}_{b\to i} \tag{A21}$$

where we used the shorthand $\Gamma_\sigma = \{b \in \partial i\backslash a : J_{b\to i} = \sigma\}$. As for equation (10), we get

$$\hat{\delta}^{(J_i)J_i}_{a\to i} = \sum_{j\in\partial a\backslash i}\prod_{l\in\partial a\backslash\{i,j\}}\left(1 - r^{(0)}_{l\to a}\right)\delta^{(-J_j)-J_j}_{j\to a} \tag{A22}$$

$$\hat{\delta}^{(0)J_i}_{a\to i} = \sum_{j\in\partial a\backslash i}\prod_{l\in\partial a\backslash\{i,j\}}\left(1 - r^{(0)}_{l\to a}\right)\delta^{(0)-J_j}_{j\to a} \tag{A23}$$

where we used the shorthand J_i, J_j for (respectively) $J_{a\to i}$ and $J_{a\to j}$. The last thing, which remains to be specified, is the coefficients $t^{(a)}_{b\to i}(q)$ entering in equations (A.18)–(A21):

$$t^{(a)}_{b\to i}(q) = \frac{1}{z[\{\hat{r}_{c\to i};\mu_1]}\sum_{\substack{\{q_c\}\\ \sum q_c = q}}\prod_{c\in\partial i\backslash\{a,b\}}\left(\hat{r}^{(q_c)}_{c\to i}\,\mathrm{e}^{-\mu_1|q_c|}\right). \tag{A24}$$

As for k-XORSAT, the recursions (A.18)–(A23) can be further simplified by restricting them to a particular linear subspace. Note in fact that the subspace $\delta^{(+)+}_{i\to a} = \delta^{(0)+}_{i\to a}$, $\delta^{(-)-}_{i\to a} = \delta^{(0)-}_{i\to a}$, $\hat{\delta}^{(J_{a\to i})J_{a\to i}}_{a\to i} = \hat{\delta}^{(0)J_{a\to i}}_{a\to i}$, is preserved by the above transformation. A numerical calculation confirms that it contains the largest eigenvalue. A further simplification occurs as $\mu_1 \to \infty$, since in this limit $t^{(a)}_{b\to i}(\pm 1) \to 0$.

Appendix B. *k*-XORSAT: expansion near the dynamic transition

In this appendix we focus on XORSAT and expand both $e_{\mathrm{d}}(\alpha)$ and $e_{\mathrm{G}}(\alpha)$ for $\alpha \to \alpha_{\mathrm{d}}$. This provides us with an analytic characterization of the dynamic transition.

Throughout this section, we shall work within the random k-XORSAT *ensemble* defined in section 3.

B.1. Dynamic energy: $e_{\mathrm{d}}(\alpha)$

Before dwelling upon the calculation, let us recall some well-known relations valid within a 1RSB approximation. The complexity can be obtained as the Legendre transform of the replicated free energy [19]:

$$\Sigma(e) = \mu e - \mu\phi(\mu) \qquad e = \frac{\partial}{\partial\mu}[\mu\phi(\mu)]. \tag{B1}$$

Since $e_{\mathrm{d}}(\alpha) \downarrow 0$ as $\alpha \downarrow \alpha_{\mathrm{d}}$, we are interested in the zero-energy (large μ) limit of the above expressions. In this limit the free energy admits an expansion of the form:

$$\mu\phi(\mu) = \phi_0 + \phi_1\,\mathrm{e}^{-2\mu} + \phi_2\,\mathrm{e}^{-4\mu} + O(\mathrm{e}^{-6\mu}). \tag{B2}$$

which implies

$$\Sigma(e) = -\phi_0 - \frac{1}{2}e\log\left(\frac{e}{-2\phi_1}\right) + \frac{1}{2}e - \frac{\phi_2}{4\phi_1^2}e^2 + O(e^3). \tag{B3}$$

The dynamical energy (and the corresponding replica-symmetry-breaking parameter) is defined as the location of the maximum of the complexity. It is therefore easy to obtain

$$e_{\rm d} = \frac{\phi_1^2}{4\phi_2} + O\left(\phi_1^4/\phi_2^2\right) \qquad \mu_{\rm d} = -\frac{1}{2}\log\left(\frac{-\phi_1}{8\phi_2}\right) + O\left(\phi_1^2/\phi_2\right). \tag{B4}$$

Let us now turn to the case of random k-XORSAT. The 1RSB variational free energy reads

$$\begin{aligned}\mu\phi(\mu) = {} & k\alpha\int {\rm d}P(r)\int {\rm d}\hat{P}(\hat{r})\log\left[1+\frac{1}{2}({\rm e}^{-2\mu}-1)(1-r_0)(1-\hat{r}_0)\right]\\ & -\alpha\int\prod_{i=1}^{k}{\rm d}P(r^{(i)})\log\left[1+\frac{1}{2}({\rm e}^{-2\mu}-1)\prod_{i=1}^{k}\left(1-r_0^{(i)}\right)\right]\\ & -\sum_{l=0}^{\infty}p_l\int\prod_{i=1}^{l}{\rm d}\hat{P}(\hat{r}^{(i)})\log\left[\sum_{q_1\dots q_l}\prod_{i=1}^{l}\hat{r}_{q_i}^{(i)}\,{\rm e}^{-\mu\sum_i|q_i|+\mu|\sum_i q_i|}\right]\end{aligned} \tag{B5}$$

where $p_l = {\rm e}^{-k\alpha}(k\alpha)^l/l!$ is the connectivity distribution of the variable nodes in the factor graph. The order parameters r and $\hat{r}$ are symmetric distributions over $\{+,0,-\}$ (which can therefore be parametrized using a single real number) and represent the distribution of the cavity fields. The functions $P(r)$ and $\hat{P}(\hat{r})$ are their distributions with respect to the disorder.

As shown in [13] and [14] it is important to distinguish the 'core' of the factor graph. Outside the core the cavity fields are trivial: $r_q = \hat{r}_q = \delta_{q,0}$. We rewrite [14]:

$$P[r] = uF[r] + (1-u)\delta[r-\delta^{(0)}] \tag{B6}$$

$$\hat{P}[\hat{r}] = \hat{u}\hat{F}[\hat{r}] + (1-\hat{u})\delta[\hat{r}-\delta^{(0)}] \tag{B7}$$

where the parameters u and $\hat{u}$ satisfy the self-consistency equations

$$\hat{u} = u^{k-1} \qquad u = 1-{\rm e}^{-k\alpha\hat{u}}. \tag{B8}$$

These equations have a non-trivial solution $u, \hat{u} > 0$ for $\alpha \geqslant \alpha_{\rm d}$.

Plugging the decomposition (B6), (B7) into equation (B5) we get:

$$\begin{aligned}\mu\phi(\mu) = {} & k\alpha u\hat{u}\int {\rm d}F(r)\int {\rm d}\hat{F}(\hat{r})\log\left[1+\frac{1}{2}({\rm e}^{-2\mu}-1)(1-r_0)(1-\hat{r}_0)\right]\\ & -\alpha u^k\int\prod_{i=1}^{k}{\rm d}F(r^{(i)})\log\left[1+\frac{1}{2}({\rm e}^{-2\mu}-1)\prod_{i=1}^{k}\left(1-r_0^{(i)}\right)\right]\\ & -(1-{\rm e}^{-k\alpha\hat{u}})\sum_{l=1}^{\infty}f_l\int\prod_{i=1}^{l}{\rm d}\hat{F}(\hat{r}^{(i)})\log\left[\sum_{q_1\dots q_l}\prod_{i=1}^{l}\hat{r}_{q_i}^{(i)}\,{\rm e}^{-\mu\sum_i|q_i|+\mu|\sum_i q_i|}\right]\end{aligned} \tag{B9}$$

where $f_l = ({\rm e}^{k\alpha\hat{u}}-1)^{-1}(k\alpha\hat{u})^l/l!$ is the connectivity distribution inside the core. The 1RSB saddle-point equations can be obtained by differentiating the above expression with respect to the distributions $F(r)$ and $\hat{F}(\hat{r})$:

$$F(r) = \sum_{l=1}^{\infty}f_l\int\prod_{i=1}^{l}{\rm d}\hat{F}(\hat{r}^{(i)})\delta[r-\rho^{\rm c}[\hat{r}^{(1)}\dots\hat{r}^{(l)}]] \tag{B10}$$

$$\hat{F}(\hat{r}) = \int \prod_{i=1}^{k-1} \mathrm{d}F(r^{(i)})\delta[\hat{r} - \hat{\rho}^{\mathrm{c}}[r^{(1)} \dots r^{(k-1)}]]. \tag{B11}$$

The saddle-point equations imply that, as $\mu \to \infty$, $F(r)$ and $\hat{F}(\hat{r})$ are supported over $r_0, \hat{r}_0 = O(\mathrm{e}^{-2\mu})$. In particular we get

$$\langle r_0 \rangle_F = \frac{f_2}{1-(k-1)f_1}\,\mathrm{e}^{-2\mu} + O(\mathrm{e}^{-4\mu}) \qquad \langle \hat{r}_0 \rangle_{\hat{F}} = \frac{(k-1)f_2}{1-(k-1)f_1}\,\mathrm{e}^{-2\mu} + O(\mathrm{e}^{-4\mu}). \tag{B12}$$

Using these results, one can expand equation (B9) for $\mu \to \infty$. We get the form (B2) with (the first two coefficients were already derived in [14]):

$$\phi_0(\alpha) = -[k\alpha u\hat{u} - \alpha u^k - k\alpha\hat{u} + (1 - \mathrm{e}^{-k\alpha\hat{u}})]\log 2 \tag{B13}$$

$$\phi_1(\alpha) = -\alpha u^k + \frac{1}{2}(k\alpha\hat{u})^2\,\mathrm{e}^{-k\alpha\hat{u}} \tag{B14}$$

$$\phi_2(\alpha) = \frac{1}{2}\alpha u^k - \frac{1}{4}(k\alpha\hat{u})^2\,\mathrm{e}^{-k\alpha\hat{u}}\left[1 - 2k\alpha\hat{u} + \frac{1}{2}(k\alpha\hat{u})^2\right] + \frac{1}{4}(k\alpha\hat{u})^5\frac{(k-1)(1-u)^2}{u[1-k(k-1)\alpha(1-u)u^{k-2}]}. \tag{B15}$$

It is easy to check that both $\phi_0(\alpha)$ and $\phi_1(\alpha)$ have finite limits $\phi_{0,\mathrm{d}}$ and $\phi_{1,\mathrm{d}}$ as $\alpha \downarrow \alpha_{\mathrm{d}}$. On the other hand, in the same limit, $\phi_2(\alpha) = \phi_{2,\mathrm{d}}(\alpha - \alpha_{\mathrm{d}})^{-1/2} + O(1)$, with

$$\phi_{2,\mathrm{d}} = \frac{1}{4}(k\alpha_{\mathrm{d}}\hat{u}_{\mathrm{d}})^4\frac{(k-1)\alpha_{\mathrm{d}}(1-u_{\mathrm{d}})}{\sqrt{2(k-1)\alpha_{\mathrm{d}}[k(k-1)\alpha_{\mathrm{d}}\hat{u}_{\mathrm{d}} - (k-2)]}} \tag{B16}$$

where we defined $u_{\mathrm{d}} = \lim_{\alpha\to\alpha_{\mathrm{d}}} u$, $\hat{u}_{\mathrm{d}} = \lim_{\alpha\to\alpha_{\mathrm{d}}} \hat{u}$. Using these expressions in equation (B4), we recover the first of the two results in (16) with $e_{\mathrm{d}}^{(0)} = \phi_{1,\mathrm{d}}^2/(4\phi_{2,\mathrm{d}})$. Moreover

$$\mu_{\mathrm{d}}(\alpha) = -\frac{1}{4}\log(\alpha - \alpha_{\mathrm{d}}) - \frac{1}{2}\log\left(\frac{-\phi_{1,\mathrm{d}}}{8\phi_{2,\mathrm{d}}}\right) + O((\alpha - \alpha_{\mathrm{d}})^{1/2}). \tag{B17}$$

One can define one more instability threshold $\mu_{1\to1}(\alpha)$ such that the 1RSB solution becomes unstable within the 1RSB space itself for $\mu < \mu_{1\to1}(\alpha)$. For $\mu < \mu_{1\to1}(\alpha)$, the 1RSB saddle-point equations can no longer be solved by a population dynamics algorithm. One has, obviously, $\mu_{1\to1}(\alpha) < \mu_{\mathrm{G}}(\alpha)$. More surprisingly, for $\alpha \gtrsim \alpha_{\mathrm{d}}$, $\mu_{\mathrm{d}}(\alpha) < \mu_{1\to1}(\alpha)$. This implies that the first expression in equation (16) cannot be directly tested against the results of a population dynamics calculation.

B.2. Stability threshold: $e_{\mathrm{G}}(\alpha)$

In order to compute the stability threshold, it is helpful to restrict ourselves to the core as in the previous section: the fluctuation parameters $\epsilon_{i\to a}$ and $\hat{\epsilon}_{a\to i}$ vanish outside. Moreover, we can work with the 'reduced' recursion (A10). It is natural to consider the behaviour of the joint probability distributions $F(r,\delta)$, $\hat{F}(\hat{r},\hat{\delta})$ under the recursions (8) and (A10). In analogy with equations (B10), (B11), we obtain

$$F(r,\delta) = \sum_{l=1}^{\infty} f_l \int \prod_{i=1}^{l} \mathrm{d}\hat{F}(\hat{r}^{(i)},\hat{\delta}^{(i)})\delta[r - \rho^{\mathrm{c}}[\{\hat{r}^{(j)}\}]]\delta\left[\delta - \sum_{i=1}^{l} t^{(i)}[\{\hat{r}^{(j)}\}]\hat{\delta}^{(i)}\right] \tag{B18}$$

$$\hat{F}(\hat{r},\hat{\delta}) = \int \prod_{i=1}^{k-1} \mathrm{d}F(r^{(i)},\delta^{(i)})\delta[\hat{r} - \rho^{\mathrm{c}}[\{r^{(j)}\}]]\delta\left[\hat{\delta} - \sum_{i=1}^{k-1} \hat{t}^{(i)}[\{r^{(j)}\}]\delta^{(i)}\right] \tag{B19}$$

where the coefficients $t^{(i)}[\cdots]$ and $\hat{t}^{(i)}[\cdots]$ are easily computed using equations (A11) and (A12). Alternatively these equations could have been derived by 'projecting' equations (2) and (3).

Note that the marginal distributions $F(r)$ and $\hat{F}(\hat{r})$ satisfy equations (B10), (B11). Therefore, if $\mu \to \infty$, $F(r,\delta)$, $\hat{F}(\hat{r},\hat{\delta})$ are supported on $r_0, \hat{r}_0 = O(\mathrm{e}^{-2\mu})$. As for $\delta, \hat{\delta}$ two cases are possible: either their support shrinks to 0 (and therefore the 1RSB solution is stable) or it remains distinct from 0. This can be checked by looking at the average value of $\delta, \hat{\delta}$ with respect to the above distributions. Using equations (B18), (B19), we get

$$\langle\delta\rangle_F = \sum_{l=1}^{\infty}\sum_{i=1}^{l} f_l \langle t^{(i)}[\{\hat{r}^{(j)}\}]\cdot\hat{\delta}^{(i)}\rangle_{\hat{F}} \qquad \langle\hat{\delta}\rangle_{\hat{F}} = \sum_{i=1}^{k-1}\langle\hat{t}^{(i)}[\{r^{(j)}\}]\cdot\delta^{(i)}\rangle_F. \tag{B20}$$

We are interested in the regime $\alpha \downarrow \alpha_{\mathrm{d}}$, $\mu_1 \uparrow \infty$, with $\mathrm{e}^{-\mu_1} \sim (\alpha - \alpha_{\mathrm{d}})$. This can be checked to be the correct scaling at the end of the computation. If we expand the above equations in this limit, we get

$$\langle\delta\rangle_F = [f_1 + 2f_2(\mathrm{e}^{-\mu_1} + 2\langle\hat{r}_0\rangle_{\hat{F}})]\langle\hat{\delta}\rangle_{\hat{F}} + O(\mathrm{e}^{-2\mu_1}) \tag{B21}$$

$$\langle\hat{\delta}\rangle_{\hat{F}} = (k-1)[1-(k-2)\langle r_0\rangle_F]\langle\delta^{(i)}\rangle_F + O(\mathrm{e}^{-2\mu_1}) \tag{B22}$$

which imply the marginality condition

$$(k-1)[1-(k-2)\langle r_0\rangle_F][f_1 + 2f_2(\mathrm{e}^{-\mu_1} + 2\langle\hat{r}_0\rangle_{\hat{F}})] = 1 + O(\mathrm{e}^{-2\mu_1}). \tag{B23}$$

Note that $\langle r_0\rangle_F$ and $\langle\hat{r}_0\rangle_{\hat{F}}$ are formally of order $\mathrm{e}^{-2\mu_1}$, cf equation (B12) but since $1-(k-1)f_1 = O(\alpha-\alpha_{\mathrm{d}})$, they must be in fact considered of order $\mathrm{e}^{-\mu_1}$. The relation can be inverted yielding

$$\mu_{\mathrm{G}}(\alpha) = -\tfrac{1}{2}\log(\alpha-\alpha_{\mathrm{d}}) - \log A + O((\alpha-\alpha_{\mathrm{d}})^{1/2}) \tag{B.24}$$

where

$$A = \frac{2(1-u_{\mathrm{d}})}{\zeta\alpha_{\mathrm{d}}u_{\mathrm{d}}}\sqrt{2(k-1)\alpha_{\mathrm{d}}[k(k-1)\alpha_{\mathrm{d}}\hat{u}_{\mathrm{d}} - (k-2)]} \qquad \zeta = 1 + \sqrt{5 - \frac{2(k-2)}{k(k-1)\alpha_{\mathrm{d}}\hat{u}_{\mathrm{d}}}}. \tag{B25}$$

Plugging this result into the general relations (B1), (B2), we get the second result in equation (16), with $e_{\mathrm{G}}^{(0)} = -2A^2\phi_{1,d}$.

Appendix C. Finite-temperature 1RSB equations

In this appendix we write explicitly the finite-temperature 1RSB cavity for greater convenience of the reader. Such equations were considered in the analysis of section 4. We limit ourselves to the case of k-SAT, generalizations being easy. The order parameter is given by a distribution over the reals $\rho_{i\to a}(h)$ or $\hat{\rho}_{a\to i}(u)$ for each directed link in the factor graph. These distributions are required to satisfy the equations

$$\rho_{i\to a}(h) = \frac{1}{\mathcal{Z}}\int\prod_{b\in\partial i\setminus a}\mathrm{d}\hat{\rho}_{b\to i}(u_b)\,\mathrm{e}^{-m\beta\Delta F(\{u_b\})}\,\delta\left(h - \sum_{b\in\partial i\setminus a}u_b\right) \tag{C1}$$

$$\hat{\rho}_{a\to i}(u) = \int\prod_{j\in\partial a\setminus i}\mathrm{d}\rho_{j\to a}(h_j)\,\delta[u - J_{a\to i}u^c(\{h_j\};\{J_{a\to j}\})] \tag{C2}$$

where

$$\Delta F(\{u_b\}) = \frac{1}{\beta}\sum_b \log 2\cosh \beta u_b - \frac{1}{\beta}\log 2\cosh\beta\left(\sum_b u_b\right) \tag{C3}$$

$$u^c(\{h_j\};\{J_j\}) = -\frac{1}{2\beta}\log\left[1 - \frac{1-\mathrm{e}^{-2\beta}}{2^{k-1}}\prod_{j=1}^{k-1}(1 - J_j\tanh\beta h_j)\right]. \tag{C4}$$

In the $T \to 0$ limit the distributions of 'hard' fields obey the same equations (C1), (C2) with the substitutions $m\beta = \mu$, and

$$\Delta F(\{u_b\}) = \sum_b |u_b| - \left|\sum_b u_b\right| \tag{C5}$$

$$u^c(\{h_j\};\{J_j\}) = \begin{cases} \min_j |h_j| & \text{if} \quad J_j h_j < 0 \quad \text{for} \quad 1 \leqslant j \leqslant k-1 \\ 0 & \text{otherwise.} \end{cases} \tag{C6}$$

As already mentioned in section 4, these $T = 0$ equations close over distributions $\rho_{i\to a}(h)$, $\hat{\rho}_{a\to i}(u)$ which are concentrated on the integers.

References

[1] Montanari A and Ricci-Tersenghi F 2003 *Eur. Phys. J.* B **33** 339
[2] Mezard M, Parisi G and Virasoro M A 1987 *Spin Glass Theory and Beyond* (Singapore: World Scientific)
[3] Dubois O, Monasson R, Selman B and Zecchina R (ed) 2001 *Theor. Comput. Sci.* **265** (special issue)
[4] Cocco S, Montanari A, Monasson R and Semerjian G 2003 Approximate analysis of search algorithms with 'physical' methods *Preprint* cs.CC/0302003
[5] Parisi G 2002 On the survey-propagation equations for the random *K*-satisfiability problem *Preprint* cs.CC/0212009
[6] Garey M R and Johnson D S 1979 *Computers and Intractability* (New York: Freeman)
[7] Monasson R, Zecchina R, Kirkpatrick S, Selman B and Troyansky L 1999 *Nature* **400** 133
[8] Biroli G, Monasson R and Weigt M 2000 *Eur. Phys. J.* B **14** 551
[9] Mézard M, Parisi G and Zecchina R 2002 *Science* **297** 812
[10] Mézard M and Zecchina R 2002 *Phys. Rev.* E **66** 056126
[11] Creignou N and Daudé H 1999 *Discrete Appl. Math.* **96–97** 41
[12] Ricci-Tersenghi F, Weigt M and Zecchina R 2001 *Phys. Rev.* E **63** 026702
[13] Cocco S, Dubois O, Mandler J and Monasson R 2003 *Phys. Rev. Lett.* **90** 047205
[14] Mézard M, Ricci-Tersenghi F and Zecchina R 2003 *J. Stat. Phys.* **111** 505
[15] Kschischang F R, Frey B J and Loeliger H-A 2001 *IEEE Trans. Inf. Theory* **47** 498
[16] Richardson T and Urbanke R 2001 *Codes, Systems, and Graphical Models* ed B Marcus and J Rosenthal (New York: Springer)
[17] Mézard M and Parisi G 2001 *Eur. Phys. J.* B **20** 217
[18] Montanari A and Ricci-Tersenghi F The asymptotic dynamics of mean-field glasses is cooling-schedule dependent (in preparation)
[19] Monasson R 1995 *Phys. Rev. Lett.* **75** 2847
[20] Gardner E 1985 *Nucl. Phys.* B **257** 747
[21] Franz S and Leone M 2003 *J. Stat. Phys.* **111** 535
[22] Monasson R 1998 *J. Phys. A: Math. Gen.* **31** 513
[23] Leuzzi L and Parisi G 2001 *J. Stat. Phys.* **103** 679
[24] Crisanti A, Leuzzi L and Parisi G 2002 *J. Phys. A: Math. Gen.* **35** 481
[25] Aspelmeier T, Bray A J and Moore M A 2003 The complexity of Ising spin glasses *Preprint* cond-mat/0309113
[26] Annibale A, Cavagna A, Giardina I, Parisi G and Trevigne E 2003 The role of the Becchi–Rouet–Stora–Tyutin supersymmetry in the calculation of the complexity for the Sherrington–Kirkpatrick model *J. Phys. A: Math. Gen.* **36** 10937
[27] Crisanti A, Leuzzi L, Parisi G and Rizzo T 2003 On spin-glass complexity *Preprint* cond-mat/0307543